Which Distance Function Use in Non-Linear Image Processing for Spectral Images?

Audrey Ledoux, Noël Richard, Anne-Sophie Capelle-Laizé and Christine Fernandez-Maloigne;
University of Poitiers, XLIM-SIC JUR CNRS 7252, Poitiers, France

Abstract

In a previous work, we developed a distance-based formalism adapted to image processing. In colour, this formalism is correlated to human perception using an adapted distance function. In this work, we extend this framework to multispectral domain. The goal is to construct an image processing formalism guided by a physical point of view. In this context, a suitable distance function between two spectra has to be specified and selected. In this paper, we specify essential characteristics of multivalued distance using two linear transformations. Different multivalued distance behaviours are compared using Gaussian distribution. Next we propose a modified distance using linear transforms. Then we compare the behaviours of different distances on real spectral images after morphological process.

Introduction

Mathematical morphology offers an attractive way to process and to analyse signals, especially image data. Morphological process allows to compute differences in spatial domain (shape, size, orientation) of objects (connected components) or to analyse image content through multiscale shape representation. Since several years, the colour or multispectral mathematical morphology extensions are widespread. Many authors developed multivalued methods but they was focused on the ordering construction without addressing a physical or perceptual sense.

In a previous work, we developed a new image processing framework distance-based function and adapted to mathematical morphology formalism. An advantage of this formalism is that the convergence coordinates are not necessary white and black colours. To extend this framework to multispectral domain, a suitable distance function between two spectra (containing the visible and/or invisible light) has to be specified and selected. This paper presents first results in this direction. In particular, we compare different distance responses to linear transforms, applied on Gaussian distributions. Then their behaviours are analysed during basic process and advanced morphological tools.

Mathematical morphology based on distance function

Many authors extend the mathematical morphology to colour or multivalued domain. The most widely used methods to define the vector expressions of minimum and maximum operators $\bigvee$ and $\bigwedge$ are two equivalent approaches, as the lexicographic order or order based on priority expressed between multivalued components [1, 2, 3]. Among the proposed approaches, the works started by Serra (Hanbury [4] followed by Lopez [5]) then continued by Aptoula [6] constitute important contributions to the colour mathematical morphology field.

But these approaches are mainly focused on the ordering construction. Moreover, most of them are basic colour extensions, issued from grayscale considerations. Using these methods, colour image converges in a multi-iterative scheme to the white during the dilation and to the black during the erosion. However with colour or multispectral images, natural convergence coordinates does not exist and these coordinates need to be expressed. Also, we propose to link colour morphological operators to the concept of *convergence*, called "Convergent Colour Mathematical Morphology" (CCMM). Thus, pixel coordinates of images are guided toward the convergence coordinates ($O^{-\infty}$ and $O^{+\infty}$) during morphological process.

The basic order relation that defines the minimum between two pixel coordinates, C_1 and C_2, in reference to the convergence coordinate $\overrightarrow{O^{-\infty}}$ for the erosion operator is:

$$C_1 \preceq C_2 \Leftrightarrow ||\overrightarrow{C_1O^{-\infty}}|| \leq ||\overrightarrow{C_2O^{-\infty}}|| \quad (1)$$

In the same way, the pixel coordinate C_1 are defined greater than C_2, in reference to the convergence coordinate $\overrightarrow{O^{+\infty}}$ for the dilation operator when:

$$C_1 \succeq C_2 \Leftrightarrow ||\overrightarrow{C_1O^{+\infty}}|| \leq ||\overrightarrow{C_2O^{+\infty}}|| \quad (2)$$

In equations (1) and (2), the vector norm $||.||$ is a distance function. To obtain a total order some additional constraints are required [7] but not used at this work level. This writing, based on distance function, is generic and allows extending the morphological operators to colour and n-dimensional data. For classical colour image processings, the only available distances are the perceptual ones such as the ΔE in the CIELAB space. However any distance is validated for spectral image processing with a perceptual or physical sense. Although the mathematical study of distribution distances on n-dimensional data is not new [8], none of authors have studied perceptual or physical sense of these distances, however essential in the spectral data use. Despite the large number of authors who are interested by multispectral tool [9] the main part of scientific works aim to reduce the complexity before any processing [10, 11, 12], reducing directly the major interest of such rich acquisition.

Constraints on distance function choice

Numerous distances exist in the literature to compare two multivalued distributions. Then the expected behaviour for the processing must be express to select the suitable distance.

Hypothesis

The goal is to determine the suitable distance function between two spectra. Behind the distance function choice, we are

looking for produce more complex image processing tools, like full-band vectorial texture features. So our questions are based on the distance accuracy and linearity behaviour in front of acquisition or content changing. So our hypothesis is that the suitable distance function is accurate and have a linear behaviour in front of linear transformations.

To illustrate our purpose on basic constraints for spectral distances, we chose a theoretical Gaussian distribution modified by two basic transformations: translation and magnification (see figure 1). The selection criteria are based on the linearity of the distance behaviour in front of both transformations (figure 2).

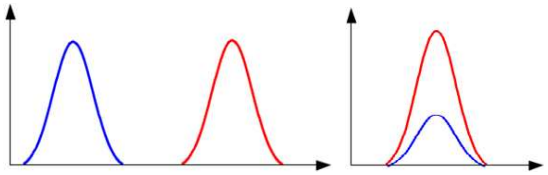

(a) Translation (b) Magnitude change

Figure 1: Spatial evolutions applied to a Gaussian distribution

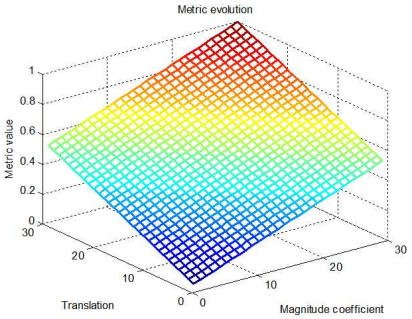

Figure 2: Distance behaviours of suitable distance depending on translation and magnitude changes

Existing distances

In this section, we compare the behaviours of some distances depending on "spatial transformation" between two synthetic distributions. Both distributions belong to R^n and are $H^1 = \{h^1_{ci}, i = 1..n\}$ and $H^2 = \{h^2_{ci}, i = 1..n\}$.

We begin with a Minkowski distance of order 2 which is the Euclidean distance. Its mathematical construction allows to obtain a linear evolution depending on magnitude transformation (see figure 3a), but it also leads to saturation with translation when both distributions have no intersection.
The Euclidean expression is given by this equation:

$$d_{L_2}(H^1,H^2) = \sqrt{\sum_{i=1}^{n}(h^1_{ci} - h^2_{ci})^2} \tag{3}$$

Next, we study the Geman-McClure distance. The distance saturates with the translation when the distributions have no intersection. The weighting applied to the distance leads to a non-linear behaviour with the magnitude changes (see figure 3b).
The Geman-McClure expression is given by this equation:

$$d_{GMC}(H^1,H^2) = \sum_{i=1}^{n}\frac{(h^1_{ci} - h^2_{ci})^2}{1 + (h^1_{ci} - h^2_{ci})^2} \tag{4}$$

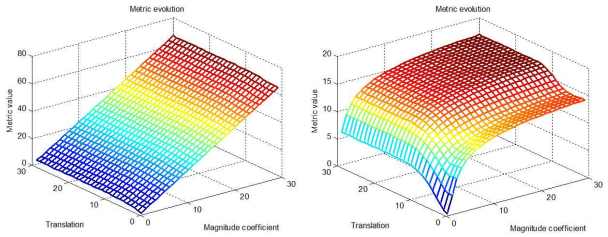

(a) Euclidean (b) Geman-McClure

Figure 3: Distance behaviours depending on translation and magnitude changes (Euclidean and Geman-McClure cases)

We continue with the Smith distance which computes an estimation of normalized overlap between two histograms. This distance saturates during the translation when the intersection between histograms is null; the saturation value is 1. The magnitude modifications have no important impact since the distance is based on the minimum function (see figure 4a).
The Smith expression is given by this equation:

$$d_{Smi}(H^1,H^2) = 1 - \frac{\sum_{i=1}^{n}\min(h^1_{ci}, h^2_{ci})}{\min\left(\sum_{i=1}^{n}(h^1_{ci}), \sum_{i=1}^{n}(h^2_{ci})\right)} \tag{5}$$

Afterward, we use the Jeffrey divergence measures the likeliness of one distribution being drawn from another one. Experiments show it saturates during the translation modifications when there is no intersection (see figure 4b). This distance obtains a linear evolution with magnitude modifications, except for low amplitudes and low translations.
The Jeffrey expression is given by this equation:

$$D_J(H^1,H^2) = \sum_{i=1}^{n}\left(h^1_{ci}\log\frac{2h^1_{ci}}{h^1_{ci}+h^2_{ci}} + h^2_{ci}\log\frac{2h^2_{ci}}{h^1_{ci}+h^2_{ci}}\right) \tag{6}$$

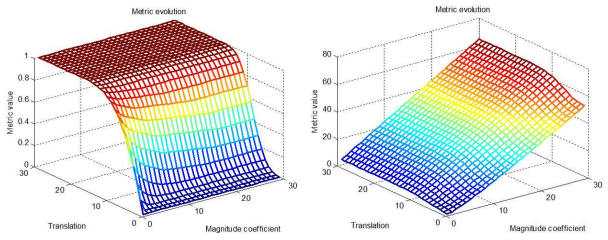

(a) Smith (b) Jeffrey

Figure 4: Distance behaviours depending on translation and magnitude changes (Smith and Jeffrey cases)

Then, we use the χ^2 distance. The initial hypothesis for this distance is that the distributions are Gaussian. Its mathematical construction leads to a saturation for translation changes when both distributions have no intersection (see figure 5a). This distance has no saturation with magnitude changes but a weakness of values due to the weighting.
The χ^2 expression is given by this equation:

$$D_{\chi^2}(H^1,H^2) = \sum_{i=1}^{n}\frac{(h^1_{ci} - h^2_{ci})^2}{(h^1_{ci} + h^2_{ci})^2} \tag{7}$$

The following distances are Bhattacharyya (see figure 5b), Divergence (see figure 6a) and Hellinger (see figure 6b) which have similar writings. These distances saturate when the distributions have no intersection and have no evolution for magnitude changes due to the normalization. In their writings $||H^p||$ is the L_1 norm of the distribution and is $d_{L_1}(H^p) = \sum_{i=1}^{n}(h_{ci}^p)$.
The Bhattacharyya expression is given by this equation:

$$D_{Bha}(H^1,H^2) = -\log\left(\sum_{i=1}^{n}\sqrt{\frac{h_{ci}^1.h_{ci}^2}{||H^1||.||H^2||}}\right) \quad (8)$$

The Divergence expression is given by this equation:

$$D_{Div}(H^1,H^2) = \sum_{i=1}^{n}\left(\left(\frac{h_{ci}^1}{||H^1||}-\frac{h_{ci}^2}{||H^2||}\right).\left(\log\frac{h_{ci}^1}{||H^1||}-\log\frac{h_{ci}^2}{||H^2||}\right)\right) \quad (9)$$

The Hellinger expression is given by this equation:

$$D_{Hel}(H^1,H^2) = 1-\sum_{i=1}^{n}\sqrt{\frac{h_{ci}^1.h_{ci}^2}{||H^1||.||H^2||}} \quad (10)$$

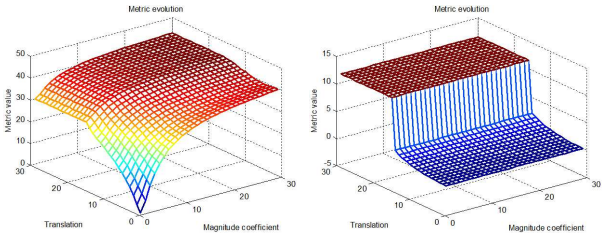

(a) χ^2 (b) Bhattacharyya

Figure 5: Distance behaviours depending on translation and magnitude changes (χ^2 and Bhattacharyya cases)

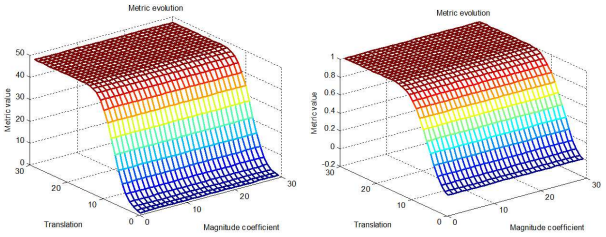

(a) Divergence (b) Hellinger

Figure 6: Distance behaviours depending on translation and magnitude changes (Divergence and Hellinger cases)

The last studied distance is the Earth Mover's Distance (EMD). It is based on the minimal cost necessary to transform one distribution into another. There is no restriction on the nature of the distributions and the dimension of both distributions can be different. The EMD computation requires cost matrix D which contains all the distances d between two components: $D_{ij} = d(h_i^1,h_j^2)$. It also requires a flow F which contains a displacements set f_{ij} that is needed to transform one distribution into another. The EMD distance is the minimization of equation 11 with a normalization (equation 12).
The EMD expression is given by this equation:

$$eq_{EMD}(H^1,H^2,F) = \sum_{i=1}^{m}\sum_{j=1}^{n}D_{ij}.f_{ij} \quad (11)$$

$$D_{EMD}(H^1,H^2) = \frac{\sum_{i=1}^{m}\sum_{j=1}^{n}D_{ij}.f_{ij}}{\sum_{i=1}^{m}\sum_{j=1}^{n}f_{ij}} \quad (12)$$

As the distance between distributions linearly increases, the energy transport cost has a linear evolution depending on translations. When the smallest distribution is full, energy transport is not possible, and then the magnitude changes do not produce value evolution. However, this energy transport is not null and decreases with respect to magnitude when translation is combined with magnitude changes (see figure 7a).

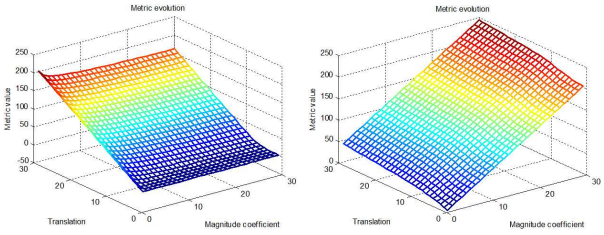

(a) EMD (b) "Combined EMD" $\alpha = 1; \beta = 1$

Figure 7: Distance behaviours depending on translation and magnitude changes (EMD and "Combined EMD" cases)

To summarize, the suitable ditance must have a linear evolution depending on translation and magnitude changes. Only the EMD distance takes into account differences during translation when distributions do not intersect. But this distance does not increase with the magnitude changes unlike Euclidean distance, Geman-McClure distance and Jeffrey divergence. However these three later distances saturate with translation changes when distributions do not intersect. The main question is: Does the suitable distance exist or should it be built?

As no suitable distance was found with the tested distances, we propose to develop a new one called "Combined EMD" close to the suitable distance. This distance is a combination between EMD and an energy difference computation (equation 13).
The "Combined EMD" expression is given by this equation:

$$D_{N_{EMD}}(H^1,H^2) = \frac{1}{\alpha}D_{EMD}(H^1,H^2)+\frac{1}{\beta}\left(||H^1||-||H^2||\right) \quad (13)$$

Figure 7b shows behaviours of this new distance and the latter evolves depending on both transformations. However the translation and the magnitude changes have different impact on the behaviours. Then in equation 13, α and β parameters are used to manage the importance of each new distance part. In figure 8a and 8b where the β parameter is respectively equal to 5 and 10, the "Combined EMD" behaviours are close to the suitable behaviours; the impact of the magnitude change is reduced.

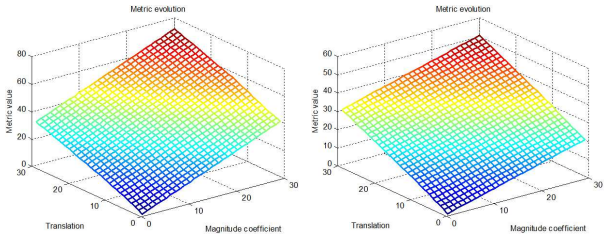

(a) "Combined EMD" $\alpha = 1; \beta = 5$ (b) "Combined EMD" $\alpha = 1; \beta = 10$

Figure 8: "Combined EMD" behaviours depending on translation and magnitude changes using different parameters

Experimental results

The previous section was dedicated to numerical comparison of multivariate distances on synthetic data and simple transformations. This section explores the impact of the previous remarks on real spectral images. We use the multispectral image database from Finlayson, Hordley and Morovic [13].

First, the distance response using 3 colour shadings extracted from a spectral images (figure 9) are compared to understand the impact of the distance selection. The spectra are corrupted with noise at their ends (figure 10). Then, to limit this noise, each spectral shading is the average computed with four columns (figure 9). Figures 11, 12 and 13 show the distance evolution between the first spectrum and each spectrum of the average shading, computed with different distances. Some differences appear between the distances in the small distance processing. Sub-figures (d) show in each case, the "Combined-EMD" and next the χ^2 approaches obtain the best dynamic range. Next, table 1 presents parameters extracted from a linear regression of the distance evolution. Even if the linear behaviour of the extracted spectral shading should be discussed, the coefficient of determination of the linear regression R^2 is good. And the results converge to select the "Combined-EMD" distances as the most adapted for spectral distances using in mathematical morphological domain.

Figure 9: Spectral image with three extracted colour shadings. Each multispectral shading is numbered. Final multispectral shadings are the average of four columns.

Second, the Beucher gradient is computed on spectral images. This gradient is obtained with one difference between dilation and erosion. Figure 14 shows results with studied distances. First remark is based on the dynamic range of gradients, as expected previously in this study, the combined EMD and χ^2 distances are more sensible. As we seen for synthetic data and basic transforms, χ^2 distance is not linear in the response. This distance filter the gradients, reducing the impact of lower ones and saturating the higher ones. To be complete, when a normalization is applied to enhance the dynamic range of all gradients, those obtained from the Euclidean distance seem similar to the EMD ones in their linear behaviour. Nevertheless, the ability to discriminate gradient using this distance should be low.

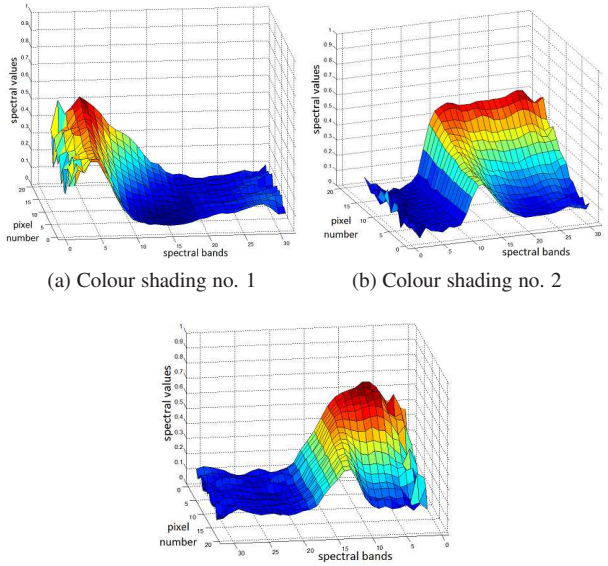

(a) Colour shading no. 1 (b) Colour shading no. 2

(c) Colour shading no. 3

Figure 10: Spectral evolution along one column of multispectral shadings

Table 1: Table of parameters for different distances

colour shading no. 1	R^2	equation
Euclidean	0.88	y=0.044x-0.11
Geman-McClure	0.72	y=0.027x-0.12
χ^2	0.87	y=0.027x-1
"Combined EMD"	0.92	y=0.44x-1.1
colour shading no. 2	R^2	equation
Euclidean	0.98	y=0.13x-0.42
Geman-McClure	0.94	y=0.19x-0.84
χ^2	0.89	y=0.65x-2
"Combined EMD"	0.977	y=0.92x-2
colour shading no. 3	R^2	equation
Euclidean	0.94	y=0.11x-0.2
Geman-McClure	0.81	y=0.14x-0.5
χ^2	0.95	y=0.31x-1.2
"Combined EMD"	0.96	y=0.73x-3.2

To complete these comparisons, we use a more complex processing tool: the hit-or-miss transform, that allows to extract objects from images [14]. As the ground truths are rare in multispectral domain, the application is focused on the search of letters in the spectral images database (Figure 15). This result ends this part of study showing best performance for approaches based on χ^2 and "Combined-EMD". Nevertheless, as in the colour case, more criteria will be required to choose or construct the most adapted distance with high confidence [7].

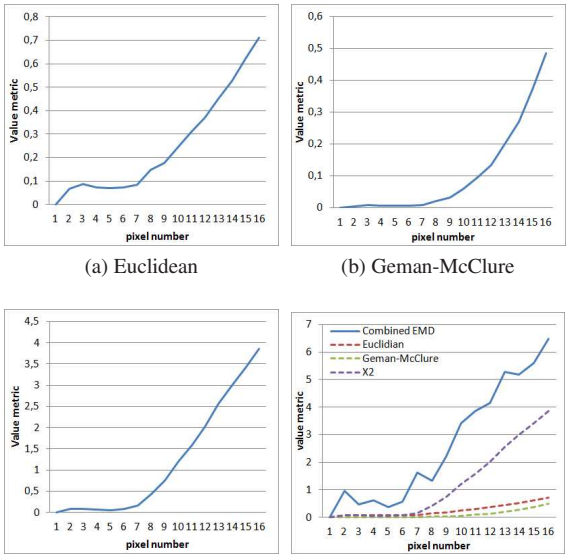

(a) Euclidean (b) Geman-McClure

(c) χ^2 (d) "Combined EMD"

Figure 11: Distance behaviour for colour shading no. 1 (mean of the 4 columns). The curves are the "distance" between the first pixel coordinates and the other pixels coordinates of the spectrum

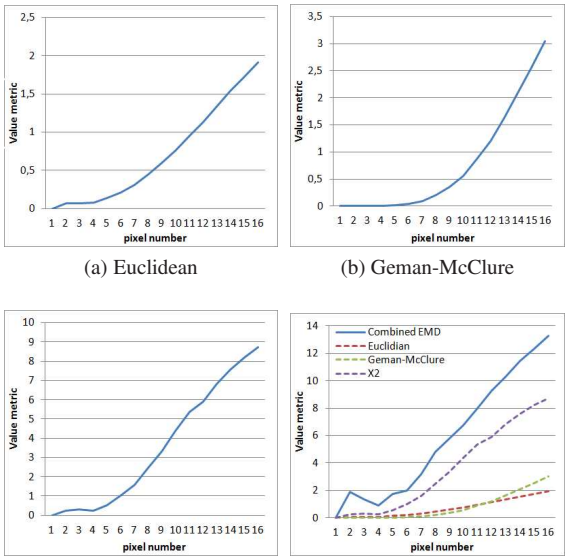

(a) Euclidean (b) Geman-McClure

(c) χ^2 (d) "Combined EMD"

Figure 12: Distance behaviour for colour shading no. 2 (mean of the 4 columns). The curves are the "distance" between the first pixel coordinates and the other pixels coordinates of the spectrum

Conclusion and perspectives

In this article, we are starting a study on the most suitable distance choice in a multispectral morphological process based on distance function. The distance choice is important in our framework to have a perceptual or physical sense. For this purpose, we compare distance behaviour in response on two linear transformations applied on a Gaussian distribution. Among the different tested distances, none evolves linearly depending on both applied transformations. With obtained results, we defined a new distance looking for be close to the suitable searched distance. The proposed distance is the closest to the expected behaviour but is not yet perfect. A result of this first part of the work is the initial question "Does the suitable distance exists or should it be built?"

Then, we compare the distance behaviour in a multispectral shading analysis and using two advanced morphological tools: Beucher gradient and hit-or-miss transform. Only the χ^2 and the proposed distance obtain a sufficient dynamic range for the Beucher gradient extraction. But the non-linearity for χ^2 distances in particular for small spectral distances should be a problem. With the second kind of morphological operators, the hit-or-miss transform, the lack of dynamic or the non-linearity in the distance behaviour shows their impacts, and only the χ^2 and 'combined-EMD' success.

However, the advanced operator computations, such as the hit-or-miss transform, stir up others questions on basis operator constructions. The linear behaviour was often cited in this work, but impossible to produce and then to enable. So to follow this work and enable the most accurate distance for spectral image processing a more complex benchmark must be developed on texture feature analysis.

Acknowledgments

This work is a part of a project MORFISM supported by L'Oréal and a project agreements State-region (FEDER).

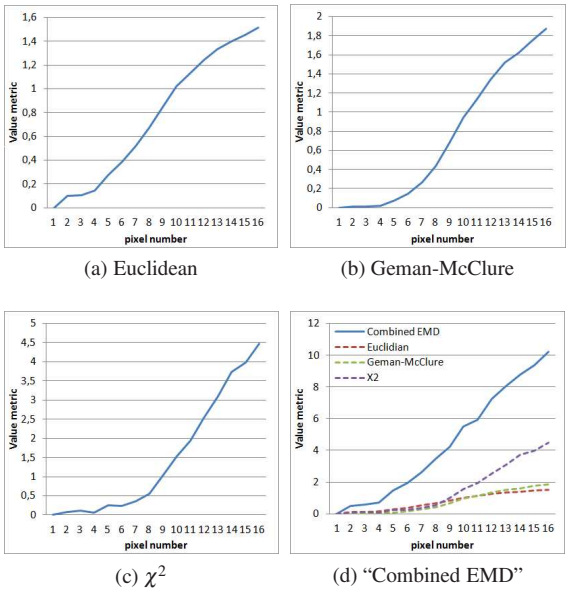

(a) Euclidean (b) Geman-McClure

(c) χ^2 (d) "Combined EMD"

Figure 13: Distance behaviour for colour shading no. 3 (mean of the 4 columns). The curves are the "distance" between the first pixel coordinates and the other pixels coordinates of the spectrum

References

[1] F. Ortiz, F. Torres, E. De Juan, and N. Cuenca, "Colour mathematical morphology for neural image analysis," *Real Time Imaging*, vol. 8, no. 6, pp. 455–465, 2002.

[2] M.C. Tobar, C. Platero, P.M. González, and G. Asensio, "Mathematical morphology in the hsi colour space," in *Pattern Recognition and Image Analysis*, pp. 467–474. Springer, 2007.

[3] P. Gonzalez, V. Cabezas, M. Mora, F. Cordova, and J. Vidal, "Morphological color images processing using distance-

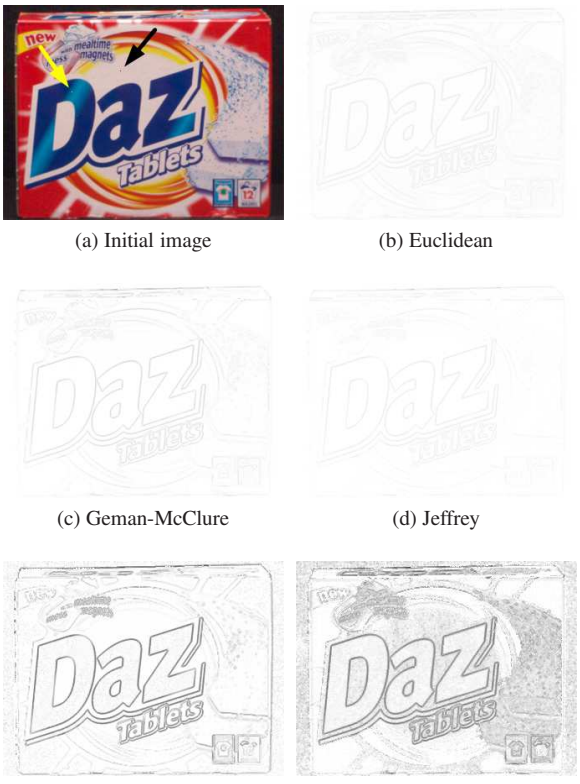

(a) Initial image (b) Euclidean

(c) Geman-McClure (d) Jeffrey

(e) χ^2 (f) "Combined EMD"

Figure 14: Multispectral Beucher gradient. The convergence points are indicated by point and arrow (yellow for the dilation and black for the erosion) in (a). Each result is multiplied by 7.

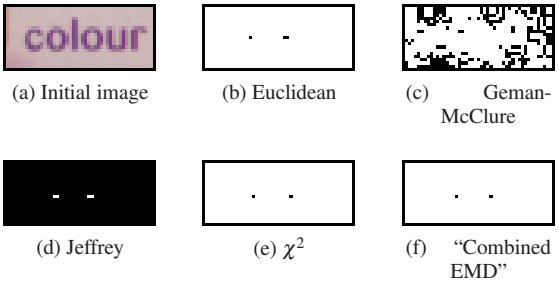

(a) Initial image (b) Euclidean (c) Geman-McClure

(d) Jeffrey (e) χ^2 (f) "Combined EMD"

Figure 15: Detection of 'o' letter

based and lexicographic order operators," in *XXIX International Conference of the Chilean Computer Science Society*. IEEE, 2010, pp. 258–264.

[4] A. Hanbury and J. Serra, "Morphological operators on the unit circle," *IEEE Transactions on Image Processing*, vol. 10, no. 12, pp. 1842–1850, 2001.

[5] J. Angulo-Lopez and J. Serra, "Morphological coding of color images by vector connected filters," in *7th International Symposium on Signal Processing and its Applications*. IEEE, 2003, vol. 1, pp. 69–72.

[6] E. Aptoula and S. Lefèvre, "A comparative study on multivariate mathematical morphology," *Pattern Recognition*, vol. 40, no. 11, pp. 2914–292, 2007.

[7] A. Ledoux, N. Richard, A.S. Capelle-Laizé, and C. Fernandez-Maloigne, "The fractal estimator: A validation criterion for the colour mathematical morphology," in *6th European Conference on Colour in Graphics, Imaging, and Vision (CGIV)*, 2012, pp. 206–210.

[8] H. Liu, D. Song, S. Rüger, R. Hu, and V. Uren, "Comparing dissimilarity measures for content-based image retrieval," *Information Retrieval Technology*, pp. 44–50, 2008.

[9] X. Wang, J.B. Thomas, J.Y Hardeberg, and P. Gouton, "Median filtering in multispectral filter array demosaicking," in *IS&T/SPIE Electronic Imaging*. International Society for Optics and Photonics, 2013, pp. 86600E–86600E.

[10] A. Plaza, P. Martinez, J. Plaza, and R. Perez, "Dimensionality reduction and classification of hyperspectral image data using sequences of extended morphological transformations," *Transactions on Geoscience and Remote Sensing*, vol. 43, no. 3, pp. 466–479, 2005.

[11] G. Noyel, J. Angulo-Lopez, and D. Jeulin, "Morphological segmentation of hyperspectral images," *Image Analysis and Stereology*, vol. 26, pp. 101–109, 2007.

[12] M. Dalla Mura, A. Villa, J.A. Benediktsson, J. Chanussot, and L. Bruzzone, "Classification of hyperspectral images by using morphological attribute filters and independent component analysis," in *2nd Workshop on Hyperspectral Image and Signal Processing: Evolution in Remote Sensing*. IEEE, 2010, pp. 1–4.

[13] G.D. Finlayson, S.D. Hordley, and P. Morovic, "Multispectral image database," http://www2.cmp.uea.ac.uk/Research/compvis/MultiSpectralDB.htm.

[14] A. Ledoux, N. Richard, and A.S. Capelle-Laizé, "Color hit-or-miss transform (cmomp)," in *20th EUropean SIgnal Processing COnference*, 2012, pp. 2248–2252.

Author Biography

Audrey Ledoux obtained his master's Degrees in signal processing from the University of Poitiers in 2010. Since, she is studying his PhD at XLIM-SIC (Signals, Images and Communications) JUR CNRS 7252 laboratory. His doctoral work is focused on the extension of mathematical morphology operators at colour based on perceptual colour distances in the CIELAB space.

Noël Richard received the Ph.D. Degrees from the University of Poitiers in 1993. Since 1992, he is researcher at XLIM-SIC. His research interests include image analysis by means of fractal geometry, colour and texture features. Since 2000, his work focuses on the colour perception of images and texture in human vision and the link between images and semantics through ontology.

Anne-Sophie Capelle-Laizé received her PhD in Image Processing from Poitiers University, France (2003). Since 2006, she is associated Professor at the University of Poitiers, France. Her work focuses on colour image processing, segmentation, data fusion and imprecise data fusion.

Christine Fernandez Maloigne is professor of signal and image processing. She manages the Department XLIM-SIC since 2008. Her actual scientific interests include image and video coding, indexing, watermarking and image quality assessment. She represents France in the Division 8 (Image Technology) of CIE and manages the TC8-12 about video and image compression assessment. She is also member of the French National Body for the ISO JPEG, since 2000.